Solid-State Electronics 54 (2010) 1566–1571

Contents lists available at ScienceDirect

Solid-State Electronics

journal homepage: www.elsevier.com/locate/sse

Modeling the input non-quasi-static effect in small signal equivalent circuit based on charge partitioning for bipolar transistors and its impact on RF noise modeling

Kejun Xia [a,b], Guofu Niu [a]

[a] Alabama Microelectronics Science and Technology Center, Electrical and Computer Engineering Department, 200 Broun Hall, Auburn University, Auburn, AL 36849, USA
[b] Maxim Integrated Products, Beaverton, OR 97005, USA

ARTICLE INFO

Article history:
Received 19 January 2010
Received in revised form 29 July 2010
Accepted 9 August 2010
Available online 30 August 2010

The review of this paper was arranged by S. Cristoloveanu

Keywords:
Noise modeling
Bipolar transistor
SiGe HBT
Non-quasi-static effect

ABSTRACT

This paper models the input non-quasi-static (NQS) effect of bipolar transistors using charge partitioning. The input NQS effect associated with the base minority carrier transport is modeled with a RC network, while the input NQS effect associated with the base-collector space charge region (CB SCR) carrier transport is modeled with a RLC network. With the proposed input NQS equivalent circuit model, *Y*-parameters and RF noise parameters using the van Vliet model are successfully modeled for frequencies up to f_T. The transport noise model is extended to represent the van Vliet model by using two noise related time constants, which eliminates the need of *Y*-parameter in the description of the noise source. The input NQS effect for such model is verified to be important only for frequencies above $f_T/3$. Analytical *Y*-parameter and noise solutions of a 1-D bipolar transistor at low injection level are used for validation.

1. Introduction

According to device physics, the base minority carrier charge in bipolar transistor (BJT) is reclaimable by both emitter and collector when V_{BE} changes [1]. This is the basic concept of charge partitioning (CP), and is further developed [2–4] for use in compact models where BJT is modeled with a collector transfer current and partitioned base charge assigned to base-emitter (BE) and base-collector (BC) branches. As shown in [2,3], both the transfer current and partitioned charge are non-quasi-static (NQS) due to the finite velocity of carrier movement and distributed nature of the quasi-neutral layers. We refer to the NQS effect of the base charge as the input NQS effect. In practice, quasi-static (QS) charge and transfer current are often used, leading to the following common emitter *Y*-parameters for minority carrier base transport

$$Y_{11}^{cp,base} = g_{be}^{base} + j\omega C_{bed}^{t}, \quad Y_{21}^{cp,base} = g_m - j\omega C_{bed}^{t}\alpha_{21}, \tag{1}$$

where g_{be}^{base} is the conductance of base current, g_m is the transconductance, C_{bed}^{t} is the total base diffusion capacitance given by $g_m\tau_b$ with τ_b being the base transit time, and α_{21} is the fraction of base charge reclaimable by the collector. Clearly the excess phase of transconductance, often referred as the output NQS effect in the literature, is modeled without the expense of any extra node. Such simplified CP model has been implemented in the industry standard compact model Mextram [5].

However, several problems exist in the simplified CP model. First, the input NQS effect is absent due to the use of QS base charge, which is particularly relevant for RF noise modeling [6,7]. As such $\Re\left(Y_{11}^{cp,base}\right) = g_{be}^{base}$ and is frequency independent, leading to implementation issues of the van Vliet noise model [8] which describes the base and collector current noises using *Y*-parameters due to minority carrier base transport

$$S_{ib}^{van,base} = 4kT\Re\left(Y_{11}^{base}\right) - 2qI_b^{base}, \tag{2}$$

$$S_{ic}^{van,base} = 4kT\Re\left(Y_{22}^{base}\right) + 2qI_c^{base}, \tag{3}$$

$$S_{icib^*}^{van,base} = 2kT\left(Y_{21}^{base} + Y_{12}^{base*} - g_m^{base}\right). \tag{4}$$

Without the input NQS effect, $S_{ib}^{van,base}$ becomes $2qI_b^{base}$ noise, a shot-like white noise, while microscopic noise calculation and measurement both show that $S_{ib}^{van,base}$ increases significantly with frequency for modern transistors [7,9]. On the other hand, S_{icib^*} has an imaginary part that grows linearly with frequency, while the real part is frequency independent, resulting in non-physical correlation. The normalized correlation can easily exceeds unity, as demonstrated

Corresponding author at: Maxim Integrated Products, 14320 SW Jenkins Road, Beaverton, OR 97005, USA. Tel.: +1 503 5451464.
E-mail address: kejun.xia@gmail.com (K. Xia).

0038-1101/$ - see front matter © 2010 Elsevier Ltd. All rights reserved.
doi:10.1016/j.sse.2010.08.002

herein. The monotonic increase of $\left|Y_{21}^{cp,base}\right|$ with frequency is neither physical nor thermodynamically sound, as pointed out in [10]. By including input NQS effect, the problem can be partially solved as shown below.

Input NQS effect models for the base have been proposed before, including Winkel's delay time model [11] which is implemented in another industry standard compact model HICUM [12], and Seitchik's single pole model [13]. The Seitchik's model is so far the most accurate NQS model, and was slightly improved by Rinaldi [14] and was extended to include the delay effect due to the collector-base space charge region (CB SCR) in [15]. However, these models are not based on charge partitioning scheme, which has advantages of fewer nodes and charge conservation [5].

In this work, we first propose a model to include both input and output NQS effects in the framework of charge partitioning for base carrier transport. For modern transistors, the transport delay in CB SCR is comparable to or even larger than the base transit time. The model is further developed to include CB SCR delay through a RLC network. We have extended the van Vliet model to include CB SCR delay [16]. We will show that the input NQS of CB SCR is critical for the extended van Vliet model. Using the proposed models, we compare noise sources and noise parameters for the extended van Vliet model with and without the input NQS effect. Using the proposed NQS model, we extend the popular transport noise model [17,18] by using two noise related delay times to reproduce the extended van Vliet model, so that noise can be accurately modeled in lack of accurate NQS *Y*-parameters. This is highly desired in practice, as inaccurate noise source, rather than inaccurate *Y*-parameters, is the main reason for the poor noise accuracy of current noise models, as we will show below. Analytical *Y*-parameter and noise solutions to the base and CB SCR of a 1-D transistor are used for verification, as NQS effects are significant at higher frequencies where experimental measurement is not available.

2. Modeling of the input NQS effect

To verify the proposed modeling method, the DC characteristics, *Y*-parameters, and noise of the quasi-neutral base are analytical solved for a 1-D NPN bipolar transistor as shown in Fig. 1 based on drift-diffusion model. The transport delay effect due to CB SCR is then taken into account by modifying both the *Y*-parameters and the noise using the method of [16]. The velocity fluctuation noise source is modeled with $4q^2D_nN(x)$ [19], where $N(x)$ is the DC electron concentration and D_n the electron diffusion coefficient. As we focus on modeling of the input NQS effect, the hot carrier effect on noise source discussed in [20] is not included for simplicity. Base built-in electric field is included to account for Ge grading, and is described with η, the total band gap grading normalized by thermal energy kT. Finite electron exit velocity at the end of base, v_{sat}, is considered. Velocity saturation effect in base is also considered through $\mu_n = \mu_{n0}/\left[1+\left(\frac{\mu_{n0}E}{v_{sat}}\right)^{\gamma}\right]^{1/\gamma}$, where $\gamma = 1.109$. The results were published in [7]. Note that neither high injection nor base push-out is considered, meaning this work focuses on biases before f_T roll off. Device geometries and process parameters are selected to achieve 230 GHz f_T at $J_c = 12.2$ mA/μm^2 and $T = 25.8$ °C. The parameters for base are $A_E = 0.12 \times 18$ μm^2, $W_B = 20$ nm, $\eta = 3.8$, $N_A = 5 \times 10^{18}$ cm^{-3}, $v_{sat} = 1.07 \times 10^7$ cm/s, electron life time $\tau_n = 154$ ns, $\mu_{n0} = 450$ cm^2/Vs given effective $\mu_n = 156$ cm^2/Vs. Ge mole fraction is 14.7% at the emitter end of the base and 28.2% at the collector end of the base. The resulting base transit time $\tau_b = 0.242$ ps. The delay time through CB SCR is $\tau_c = 0.38$ ps. The resulting f_T of the base and CB SCR, defined as $1/2\pi(\tau_b+\tau_c)$, is 256 GHz. To make a realistic device such as the raised-base SiGe HBT as shown in [21], we add extra base current injected into the emitter through $\beta = 100$, BE depletion capacitance $C_{bej} = 43$ fF, BC depletion capacitance $C_{bcj} = 27$ fF, base resistance $r_b = 5\ \Omega$, and emitter resistance $r_e = 1.6\ \Omega$. These RC elements are representative of a 250 GHz SiGe HBT technology. For illustration, we will use an external $V_{BE} = 0.926$ V, with $f_T = 230$ GHz at $J_c = 12.2$ mA/μm^2.

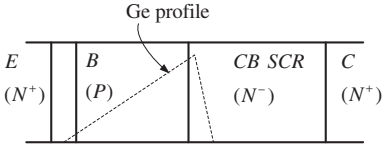

Fig. 1. The structure of an ideal 1-D NPN bipolar transistor with triangle Germanium doping in base.

2.1. The input NQS effect for the quasi-neutral base based on charge partitioning

First, we review Seitchik's NQS model [13] shown in Fig. 2a. Base depletion capacitance C_{bej} is not considered here, as it is quasi-static for all practical purpose, and will be added later. r_d^t represents the input NQS effect of the base minority charge and $\tau_2 = r_d^t C_{bed}^t$. τ_1 is the extra delay time of the collector current, and is approximated with a RLC network as shown in the dashed box of Fig. 2a. The *Y*-parameters are

$$Y_{11}^{seitchik,base} = g_{be}^{base} + \frac{j\omega C_{bed}^t}{1+j\omega\tau_2}, \quad Y_{21}^{seitchik,base} = \frac{g_m e^{-j\omega\tau_1}}{1+j\omega\tau_2}. \tag{5}$$

The collector current responds to the supplied v_{be} by a total output delay time τ_d as

$$\tau_d = \tau_1 + \tau_2. \tag{6}$$

Equating the imaginary part of $Y_{21}^{seitchik,base}$ in (5) and $Y_{21}^{cp,base}$ in (1) at low frequencies, we obtain $\alpha_{21} = \tau_d/\tau_b$. Note τ_b, τ_d and τ_2 (so that τ_1 and α_{21}) can be analytically solved at arbitrary injection level following [14]. At low injection level, one has the following results for narrow base with negligible recombination

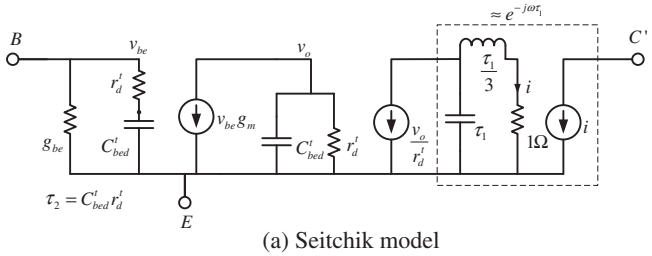

(a) Seitchik model

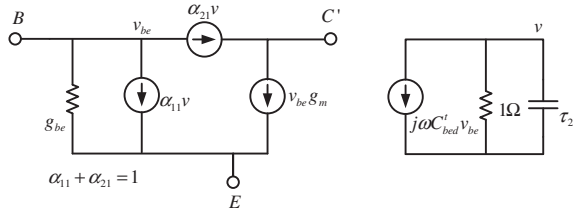

(b) Charge partitioning model proposed

Fig. 2. Small signal equivalent circuit for quasi-neutral base including the input NQS effect. (a) Seitchik's model. (b) Proposed charge partitioning model.

$$\tau_b = \frac{\eta - 1 + e^{-\eta}}{\eta^2}\frac{d_B^2}{D_n} + \frac{1 - e^{-\eta}}{\eta}\frac{d_B}{v_{sat}}, \tag{7}$$

$$\tau_d \approx \tau_b \frac{\eta\coth(\eta/2) - 2}{\eta - 1 + e^{-\eta}}, \tag{8}$$

$$\tau_2 \approx \tau_b \left[\frac{\eta\coth(\eta/2) + 1 + \eta}{\eta - 1 + e^{-\eta}} - \frac{3}{2}\frac{\eta^2}{(\eta - 1 + e^{-\eta})^2}\right]. \tag{9}$$

Eqs. (8) and (9) are exact when $v_{sat} \to \infty$ [11], and are good approximations for finite v_{sat} [7]. Fig. 2a accurately models Y_{11} and Y_{21} up to $1/(2\pi\tau_b)$ as evaluated in [14]. However, *four* extra nodes have been added to model both the input and output NQS effects.

Fig. 2b shows the proposed NQS equivalent circuit based on charge partitioning. The input NQS effect is modeled with a RC network where $R = 1\ \Omega$ and $C = \tau_2$. α_{11} is the fraction of charge reclaimed by the emitter and $\alpha_{21} + \alpha_{11} = 1$. Only *one* extra node is needed to model both input and output NQS effects. Fig. 2b is more computationally efficient than Fig. 2a.

The Y-parameters of the CP equivalent circuit are

$$Y_{11}^{cp-new,base} = g_{be}^{base} + \frac{j\omega C_{bed}^t}{1 + j\omega\tau_2}, \tag{10}$$

$$Y_{21}^{cp-new,base} = g_m - \frac{j\omega g_m \tau_d}{1 + j\omega\tau_2}. \tag{11}$$

Clearly, the new CP model accurately models Y_{11}^{base} since $Y_{11}^{cp-new,base} = Y_{11}^{seitchik,base}$. To analyze the difference of Y_{21}^{base}, we compare the Taylor expansion of (5), (11), and their magnitudes to the second order of ω,

$$Y_{21}^{seitchik,base} \approx -j\omega g_m\tau_d + g_m[1 - \omega^2(\tau_d^2 + \tau_2^2)/2], \tag{12}$$

$$Y_{21}^{cp-new,base} \approx -j\omega g_m\tau_d + g_m[1 - \omega^2\tau_d\tau_2], \tag{13}$$

$$\left|Y_{21}^{seitchik,base}\right| \approx g_m(1 - \omega^2\tau_2^2/2), \tag{14}$$

$$\left|Y_{21}^{cp-new,base}\right| \approx g_m[1 - \omega^2\tau_d(\tau_2 - \tau_d/2)]. \tag{15}$$

One can observe that

- As expected, including the input NQS effect in the CP model does not modify the imaginary part of Y_{21}^{base} to the first order of ω.
- After including the input NQS effect in the CP model, the real part of Y_{21}^{base} now rolls off versus frequency. However, the roll-off is less than Seitchik's model, because $\tau_2 \geqslant \tau_d/2$ which can be proved for any η based on (8) and (9).
- Similarly, the magnitude of Y_{21}^{base} rolls off versus frequency for the proposed CP model. Again, the roll-off is underestimated compared to Seitchik's. Nevertheless, including the input NQS effect alleviates the thermodynamics difficulty discussed earlier for the simplified CP model. For modern transistors, the Y_{21} roll-off is dominated by CB SCR effect, because of increasing importance of CB SCR transit time compared to base transit time. Therefore, the underestimation in the base region is not a practical issue.

2.2. The input NQS effect for CB SCR

Carrier transport through CB SCR modifies both the Y-parameters and the noises of base and collector [16]. We denote τ_c as the delay time through CB SCR. The resulting Y-parameters are [22]

$$Y_{11}^{intr} = Y_{11}^{base} + Y_{\tau_c}, \tag{16}$$

$$Y_{21}^{intr} = \lambda Y_{21}^{base} = Y_{21}^{base} - Y_{\tau_c}, \tag{17}$$

where

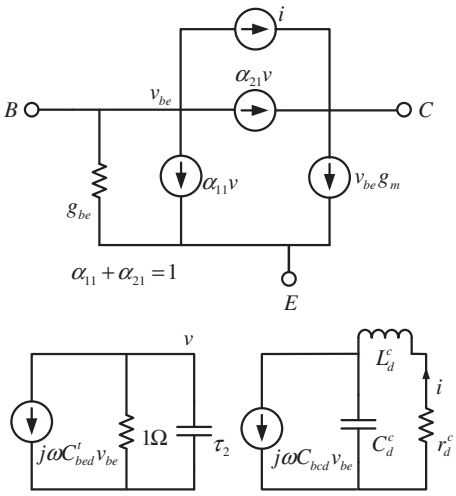

Fig. 3. Proposed small signal equivalent circuit for quasi-neutral base and CB SCR including the input NQS effect.

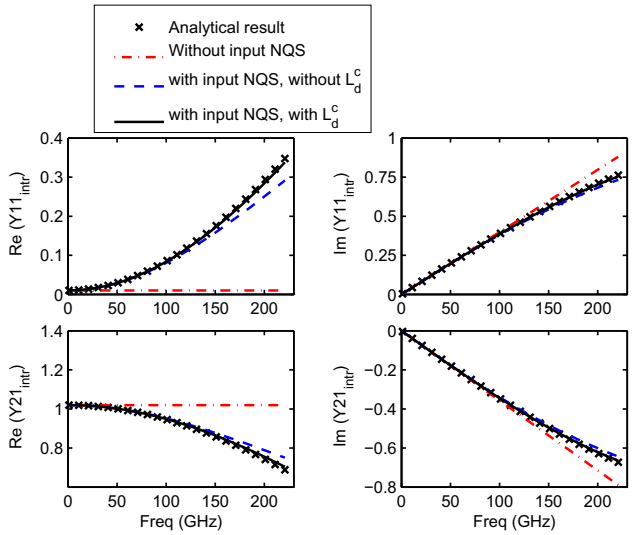

Fig. 4. Y-parameters of quasi-neutral base and CB SCR. $J_c = 12.2$ mA/μm^2. $A_E = 0.12 \times 18$ μm^2.

$$Y_{\tau_c} \equiv (1 - \lambda)Y_{21}^{base}, \quad \lambda = \frac{1 - e^{-2j\omega\tau_c}}{2j\omega\tau_c}. \tag{18}$$

A first order approximation of Y_{τ_c} is $j\omega C_{bcd}$ where $C_{bcd} = g_m\tau_c$. It means that Y_{τ_c} can be modeled to the first order with another transcapacitance between the base and the collector, or in terms of charge partitioning, the charge in the CB SCR is entirely reclaimed by the collector.

We propose to model the input NQS effect of C_{bcd} with a RLC network shown in Fig. 3. The elements are r_d^c, L_d^c, and C_d^c. Fig. 3 produces a Y_{τ_c} of

$$Y_{\tau_c,model} = \frac{j\omega C_{bcd}}{1 + j\omega r_d^c C_d^c - \omega^2 L_d^c C_d^c}. \tag{19}$$

Comparing (19) to (18) to the third order of ω, we can determine

$$r_d^c = \frac{2}{3} + \frac{\tau_d}{\tau_c}, C_d^c = \tau_c, \quad L_d^c \approx \frac{\tau_c}{9} + \frac{2}{3}\tau_d. \tag{20}$$

The input NQS delay time of CB SCR is

$$\tau_{cnqs} = r_d^c C_d^c = \frac{2}{3}\tau_c + \tau_d. \tag{21}$$

Fig. 4 shows the calculated Y-parameters including both base and CB SCR carrier transport calculated using different models, (1) Analytical results in x symbols from the AC solution of transport equation. (2) The equivalent circuit of Fig. 3, but without the two input NQS networks, represented by dot-dashed curves. (3) Full circuit of Fig. 3, represented by solid curves. (4) Fig. 3 without the inductance L_d^c, represented by dashed curves. Note that the base current injected into the emitter is included in the calculation, that is $g_{be} = g_{be}^{base} + qI_b^e/(kT)$. The NQS effect of this current is negligible [16].

The proposed NQS equivalent circuit achieves good accuracy up to $1/[2\pi(\tau_b + \tau_c)]$, the f_T of the intrinsic transistor. Without input NQS, the frequency dependences of $\Re\left(Y_{11}^{intr}\right)$ and $\Re(Y_{21}^{intr})$ are totally ignored, which corresponds to the current CP model implemented in Mextram.

The proposed NQS model uses *three* external nodes, hence has one less node than the Seitchik's model. One may consider not including the inductance L_d^c to save one more node. Comparing the dashed and solid curves in Fig. 4, we observe that the inductance notably improves the modeling accuracy at frequencies above $f_T/2$ for both $\Re\left(Y_{11}^{intr}\right)$ and $\Re\left(Y_{21}^{intr}\right)$. More importantly, the pure time delay τ_c is best described by a RLC network, especially for large signal modeling [23]. Therefore, we suggest using RLC network to model the input NQS effect of CB SCR. Although less nodes usually result in reduction of circuit simulation time, further testing of the proposed model in large signal model is necessary to evaluate its efficiency when comparing with other models.

2.3. Noise sources of the intrinsic transistor

To illustrate the impact of input NQS effect on noise modeling, we calculate base and collector current noises and their correlation from Y-parameters obtained with and without input NQS effect, using the extended van Vliet model [16]. The resulting noise current spectrums S_{ib}, S_{ic} and normalized correlation c $\left(\triangleq S_{icib^*}/\sqrt{S_{ib}S_{ic}}\right)$ are shown in Fig. 5. The analytical noise solution from Langevin equation [7], labeled as" analytical results" and shown in x symbol, is used as reference. Also shown is an extended transport noise model developed below for the purpose of modeling noise sources accurately when NQS Y-parameters are not available or difficult to extract, which is often the case in practice.

The extended van Vliet model is an extension of the original van Vliet model given by (2)–(4) to modern transistors by including CB SCR carrier transport [16]

$$\begin{aligned}
S_{ib}^{van} &= \{4kT\Re\left(Y_{11}^{intr}\right) - 2qI_b\} + 2qI_c|1-\lambda|^2 - 4kTg_m\Re(1-\lambda),\\
&\approx \left\{4kT\Re\left(Y_{11}^{intr}\right) - 2qI_b\right\} - 2qI_c(1-|\lambda|^2),\\
S_{icib^*}^{van} &= \left\{2kT\left(Y_{21}^{intr} + Y_{12}^{intr*} - g_m\right)\right\} + 2qI_c(\lambda - |\lambda|^2) + 2kTg_m(1-\lambda),\\
&\approx \left\{2kT\left(Y_{21}^{intr} + Y_{12}^{intr*} - g_m\right)\right\} + 2qI_c(1-|\lambda|^2),\\
S_{ic}^{van} &= \{2qI_c\}|\lambda|^2,
\end{aligned} \tag{22}$$

where the approximation is realistic when $g_m \approx qI_c/(kT)$. The solid curves represent the extended van Vliet model which agree with the analytical results quite well for frequencies up to f_T.

Since the van Vliet model relies on the intrinsic Y-parameters to model the noise source, the input NQS effect directly influences noise modeling. Without including the input NQS effect in the equivalent circuit, the extended van Vliet model gives unphysical results, as shown by the dot-dashed curves. S_{ib} is white $2qI_b$ at low frequencies, and becomes negative at higher frequencies due to the negative $-2qI_c(1-|\lambda|^2)$ term in S_{ib}^{van} of (22). Consequently, the Cauchy-Schwarz inequality $S_{ib}S_{ic} \geqslant |S_{icib^*}|^2$ or $|c| \leqslant 1$ [24] is violated for frequencies above 30 GHz, as either $\Re(c) > 1$ or $\Im(c) > 1$. Even without the $-2qI_c(1-|\lambda|^2)$ term, that is, using the original van Vliet model as is for both base and CB SCR, violates the Cauchy-Schwarz inequality within such frequency range.

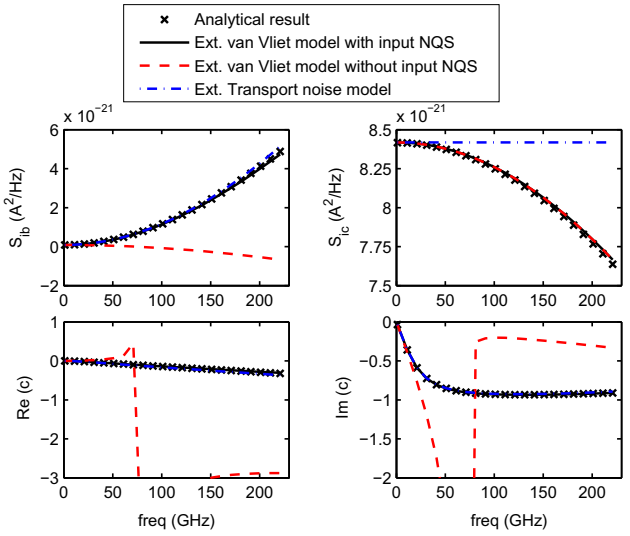

Fig. 5. Base and collector current noise of quasi-neutral base and CB SCR. $J_c = 12.2$ mA/μm^2. $A_E = 0.12 \times 18$ μm^2.

The strength of the van Vliet model and the extended van Vliet model lies in the fact that noise sources are described using Y-parameters due to base and CB SCR carrier transport. Therefore, in principle, one can achieve noise modeling without using any model dedicated model parameter for noise. In practice, this is extremely difficult. Experimentally measured Y-parameters inevitably include effects of parasitic elements like base resistance, making the extraction of NQS intrinsic Y-parameters difficult. It is for this reason that in practice, noise sources are often described independently from Y-parameters using dedicated modeling equations involving the use of dedicated parameters. One popular model is the transport model [17,18]. That model, however, is not sufficiently accurate. We propose here an extension of the transport noise model

$$S_{ib}^{tran} = 2qI_b + 4qI_c\left[1 - \Re\left(e^{j\omega\tau_n^b}\right)\right], \tag{23}$$

$$S_{ic}^{tran} = 2qI_c, \tag{24}$$

$$S_{icib^*}^{tran} = 2qI_c(e^{-j\omega\tau_n^c} - 1). \tag{25}$$

In the original transport model [17,18], only one noise delay time is used, i.e., $\tau_n^b = \tau_n^c = \tau_n$. Here the two noise delay times are chosen to reproduce the S_{ib}, S_{ic} and S_{icib^*} of the extended van Vliet model shown in (22) up to second order of ω. This leads to

$$\tau_n^b = \sqrt{\tau_c^2 + 2\tau_c\tau_d + 2\tau_b\tau_2}, \tag{26}$$

$$\tau_n^c = \tau_d + \tau_c. \tag{27}$$

One can prove that $\tau_n^b > \tau_n^c$ based on the fact $\tau_2 \geqslant \tau_d/2$, which guarantees $|c| \leqslant 1$. As shown in Fig. 5, the extended transport noise model accurately models S_{ib} and $\Im(c)$, and is reasonably good for $\Re(c)$ and S_{ic}.

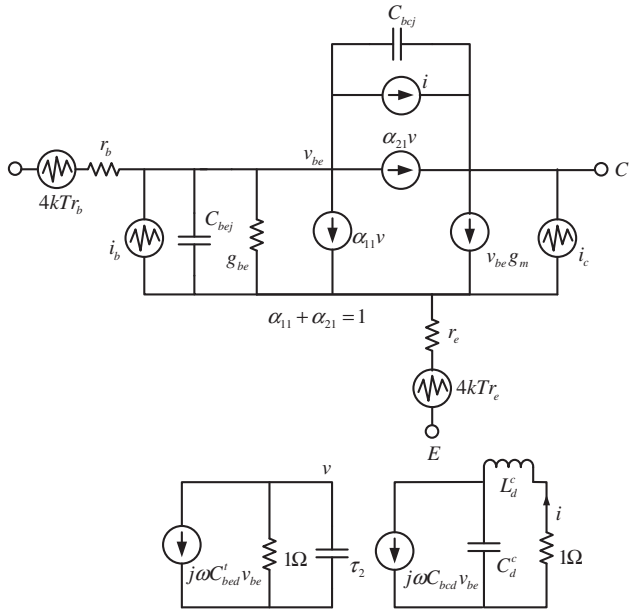

Fig. 6. Small signal equivalent circuit for the whole transistor with noise sources.

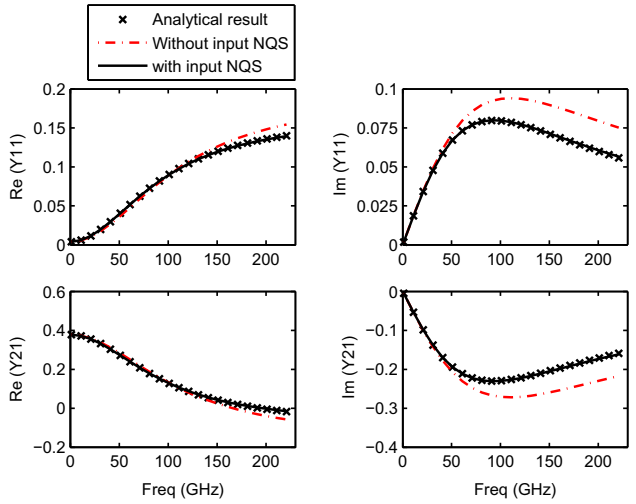

Fig. 7. Y-parameters of the whole transistor. External V_{BE} = 0.926 V. J_c = 12.2 mA/μm^2. A_E = 0.12 × 18 μm^2.

3. Input NQS effect on the Y and noise parameters for the whole transistor

We now add the BE and BC depletion capacitances, the base and emitter resistances. Fig. 6 shows the resulting small signal equivalent circuit for the whole transistor with noise sources. Note that all resistors representing delay time are noiseless.

Fig. 7 shows the Y-parameters of the whole transistor. The x symbols represent analytical results. The solid curves are calculated by including the input NQS effect. Obviously, the proposed model predicts the analytical results accurately for frequencies up to f_T. The dot-dashed curves are calculated without the input NQS effect, or the two input NQS effect networks in Fig. 6 are ignored. The input NQS effect reduces the admittances for $f > f_T/3$, especially $\Im(Y_{11})$ and $\Im(Y_{21})$. Comparing with Fig. 4, we observe that adding r_b significantly reduces the difference of $\Re(Y_{11})$ between with and without the input NQS effect. This explains in part why pure extraction of input NQS has been difficult, particularly when the frequency of data is not high enough. This also confirms the usage of the extended transport noise model in practice. Below we emphasize that the noise source of van Vliet model is determined by Y^{int} shown in Fig. 4, not by Y^{whole} in Fig. 6.

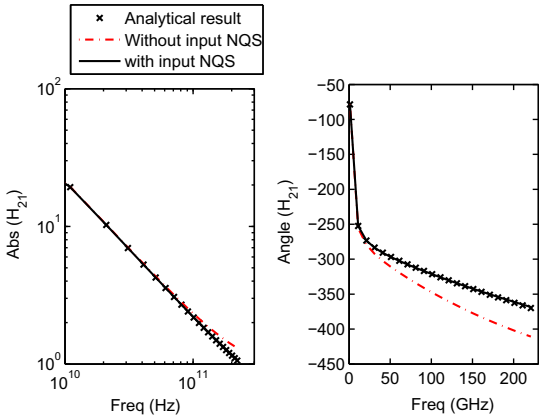

Fig. 8. H_{21} of the whole transistor. External V_{BE} = 0.926 V. J_c = 12.2 mA/μm^2. A_E = 0.12 × 18 μm^2.

Fig. 8 shows the AC current gain H_{21} ($\equiv Y_{21}/Y_{11}$) of the whole transistor. The curves have the same meanings as Fig. 7. Without the input NQS effect modeled, both the magnitude and the angle are noticeably overestimated for frequencies above $f_T/3$.

Fig. 9 show the noise parameters of the whole transistor. The x symbols represent the analytical results. The solid curves are the extended van Vliet model with the input NQS effect modeled. As such, the implementation of the extended van Vliet model becomes physical, all of the four noise parameters are well modeled, for frequencies up to f_T. The solid curves with circle symbols are the van Vliet model without the input NQS effect modeled. Clearly, the van Vliet model only works for frequencies up to several GHz where $\Re(Y_{11})$ is close to g_{be}. At higher frequencies, the noise parameters are totally wrong due to the violation of the Cauchy-Schwarz inequality discussed previously.

The dashed curves in Fig. 9 are the extended transport noise model with the input NQS effect modeled. The model is almost as accurate as the van Vliet model for all four noise parameters,

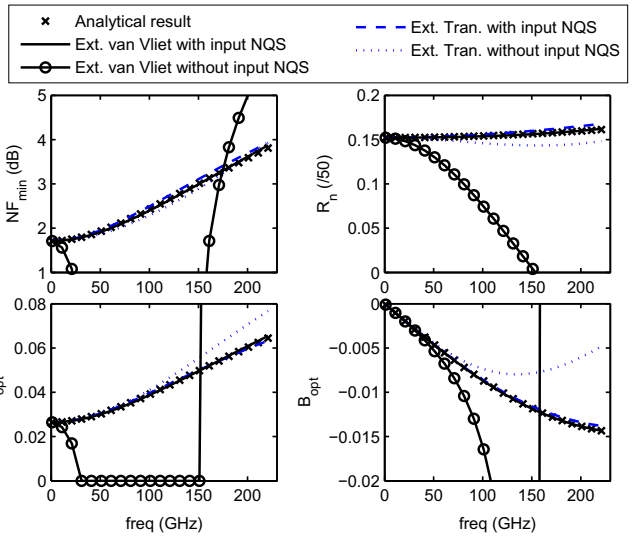

Fig. 9. Noise parameters of the whole transistor. External V_{BE} = 0.926 V. J_c = 12.2 mA/μm^2. A_E = 0.12 × 18 μm^2.

due to its good description of the intrinsic noise source shown in Fig. 5. The dotted curves represent the extended transport noise model without the input NQS effect. Unlike the van Vliet model, transport noise model does not rely on the *Y*-parameters to describe the noise source, therefore there is no numerical problem for the full frequency range. Interestingly, NF_{min} is almost as accurate as the case of with the input NQS effect for frequencies up to f_T. Other three parameters are reasonably accurate up to $f_T/3$. At frequencies above $f_T/3$, R_n is underestimated by up to 7%; G_{opt} is overestimated by up to 10%; B_{opt} is significantly underestimated by up to 50%. Including the input NQS effect in equivalent circuit is important only for frequencies higher than $f_T/3$, as long as the noise sources are separately modeled accurately, as in the case of using the extended transport noise model. Such fact suggests that the main issue with improving noise parameter modeling accuracy still lies in noise source modeling. All the above conclusions about how the input NQS effect impact on noise are valid for different values of external resistances and depletion capacitances.

4. Conclusions

Equivalent circuit model with both input and output NQS effects has been developed to describe carrier transport in both base and CB SCR. The input NQS effect affects *Y*-parameters at frequencies higher than $f_T/3$. An extended transport noise model is developed which is useful in practice because input NQS effect is hard to extract from measured *Y*-parameters. Both the extended van Vliet model and the extended transport noise model provide accurate noise modeling results for frequencies up to f_T when the input NQS effect is modeled. Without the input NQS effect in the equivalent circuit, the van Vliet model suffers numerical problem and only works for frequencies around several GHz. The extended transport noise provides reasonably accurate results for frequencies up to $f_T/3$.

References

[1] Lindmayer J, Wrigley CY. Fundamentals of semiconductor devices. Princeton (NJ): Van Nostrand; 1965.

[2] Fossum JG, Veeraraghavan S. Partition charge based modeling of bipolar transistor for non-quasi-static circuit simulation. IEEE Electron Dev Lett 1986;7(12):652–4.

[3] Klose H, Wieder AW. The transient integral charge control relation – a novel formulation of the currents in a bipolar transistor. IEEE Electron Dev Lett 1987;34(5):1090–9.

[4] Jeong H, Fossum JG. A charge-based large-signal bipolar transistor model for device and circuit simulation. IEEE Trans Electron Dev 1989;36(1):124–31.

[5] Paasschens JCJ, van der Toorn R, Kloosterman WJ. Manual for Mextram bipolar transistor model, the NXP. <http://www.nxp.com/models/bi_models/mextram>.

[6] Xia K, Niu G, Sheridan D, Sweeney S. Input non-quasi static effect on small signal parameter extraction and noise modeling for SiGe HBTs. In: Proceedings of the IEEE BCTM; October 2005. p. 180–3.

[7] Xia K. Improved RF noise modeling for silicon–germanium heterojunction bipolar transistors. PhD dissertation, Auburn University; 2006. <http://etd.auburn.edu/etd/handle/10415/610?show=full>.

[8] van Vliet KM. General transport theory of noise in pn junction-like devices-I. Three-dimensional green's function formulation. Solid State Electron 1972;15:1033–53.

[9] Xia K, Niu G, Sheridan D, Sweeney S. Frequency and bias-dependent modeling of correlated base and collector current RF noise in SiGe HBTs using quasi-static equivalent circuit. IEEE Trans Electron Dev 2006;53(3):515–22.

[10] Chen MK, Lindholm FA, Wu BS. Comparison and extension of recent one-dimensional bipolar transistor models. IEEE Trans Electron Dev 1988;35(7):1096–106.

[11] Winkel JT. Extended charge-control model for bipolar transistor. IEEE Trans Electron Dev 1973;20(4):389–94.

[12] Schroter M, Mukherjee M. Manual for Hicum bipolar transistor model. Technische Universitat Dresden. <http://www.iee.et.tu-dresden.de/iee/eb/hic_new/hic_modtest.html>.

[13] Seitchik JA, Chatterjee A, Yang P. An accurate bipolar model for large signal and ac applications. IEDM Tech Dig 1987:244–7.

[14] Rinaldi NF, deGraaff HC, Tauritz JL. Analysis and modeling of small-signal bipolar transistor operation at arbitrary injection levels. IEEE Trans Electron Dev 1999;45(8):1817–25.

[15] Rinaldi NF. Modeling of collector signal delay effects in bipolar transistors. Solid State Electron 1999;43:359–65.

[16] Xia K, Niu G. Discussions and extension of van Vliet's noise model for high speed bipolar transistors. Solid State Electron 2009;53(3):349–54.

[17] Niu G, Cressler JD, Zhang S, Ansley WE, Webster CS, Harame DL. A unified approach to RF and Microwave noise parameter modeling in bipolar transistors. IEEE Trans Electron Dev 2001;48(11):2568–74.

[18] Rudolph M, Doerner R, Klapproth L, Heymann P. An HBT noise model valid up to transit frequency. IEEE Electron Dev Lett 1999;20(1):24–6.

[19] Shockley W, Copeland JA, James RP. The impedance-field method of noise calculation in active semiconductor device. In: Lowdin PO, editor. Quantum theory of atoms, molecules, and the solid state. Newyork: Academic; 1966. p. 537–63.

[20] Nougier JP. Fluctuations and noise of hot carriers in semiconductor materials and devices. IEEE Trans Electron Dev 1994;41(12):2034–49.

[21] Freeman G, Jagannathan B, Jeng SJ, Rieh JS, Stricker A, Ahlgren D, et al. Transistor design and application considerations for >200-GHz SiGe HBTs. IEEE Trans Electron Dev 2003;50(3):645–55.

[22] Reisch M. High-frequency bipolar transistors. Springer Series in Advanced Microelectronics. Berlin (Germany): Springer Verlag; 2002.

[23] Weil PB, McNamee LP. Simulation of excess phase in bipolar transistors. IEEE Tran Circ Syst 1978;26(2):114–6.

[24] Paasschens JCJ, Havens RJ, Tiemeijer LF. Modeling the correlation in the high-frequency noise of (hetero-junction) bipolar transistors using charge partitioning. In: Proceedings of the IEEE BCTM; 2003. p. 221–4.